TAO, Supplementary Issue, 115-126, March 1999

The Effect of the Atmosphere on the OCI Channels: Rayleigh Scattering

Wann-Jin Chen[1], Chung-Yi Tseng[2], Gin-Rong Liu[3] and Shih-Jen Huang[3]

(Manuscript received 10 December 1998, in final form 29 January 1999)

ABSTRACT

One of the key issues for ocean color investigation using Ocean Color Imager (OCI) radiance is the correction for atmospheric effect. In particular, the water-leaving radiance is an order of magnitude less than that of observed radiance, so the accuracy of the concentration of phytoplankton pigments retrieval depends on the accuracy of the correction of atmospheric effect. According to the magnitude of atmospheric effect, it is divided into three categories: the zero order, Rayleigh scattering; the first order, Mie scattering; the second order, including the effect of multi-scattering, polarization, sea surface roughness, viewing angle and the temporal and spatial variation of pressure and total ozone concentration. The Rayleigh scattering effect on OCI channels is the focus of this paper. The optical thickness of Rayleigh scattering and the transmittance of the atmosphere were calculated using 5 coastal surface data from the Taiwan area. The results show that the optical thickness of Rayleigh scattering and the transmittance of the atmosphere are significantly changed for various locations and seasons. To ensure that the atmospheric model can be used in operation, a model for providing Rayleigh scattering optical thickness and transmittance has been established using three-year surface data.

The daily and seasonal variations of Rayleigh scattering radiance were discussed. In daily variation, the results show that before noon the minimum regions of Rayleigh scattering radiance spread from the center to the edge in the Rayleigh radiance image and after noon the minimum regions of Rayleigh scattering radiance come together from the edge to the center. The reason for these phenomena may be caused by different solar zenith angles. In seasonal variation, it was found that the Rayleigh scattering radiance was significantly changed following the declination movement of

[1]Department of Applied Physics, Chung Cheng Institute of Technology, Ta-Shi, Tao-Yuan, Taiwan, ROC

[2]Institute of Physics, Academia Sinica, Taipei, Taiwan, ROC

[3]Center for Space and Remote Sensing Research, National Central University, Chung-Li, Tao-Yuan, Taiwan, ROC

the sun. Generally, the Rayleigh scattering radiance in winter is less than that in summer. In addition, the minimum value, the maximum value and the range of Rayleigh scattering radiance were discussed. In daily variation, the results indicate that among the maxima, the radiance at 8 A.M. is largest, and among the minima, the radiance at 10 A.M. is smallest, and that within the range the difference at 8 A.M. is largest, and at 10 A.M. is smallest. In seasonal variation, the results show that among the minima, January is largest and among the maxima, June is the smallest. The Rayleigh scattering radiance regularly increases from January to June and regularly decreases from June to December and the minimum range occurs in March and maximum range in June.

(Key words: OCI, Atmospheric correction, Rayleigh scattering, Optical thickness)

1. INTRODUCTION

There have been two decades of ocean color investigation by satellite sensing. The Coastal Zone Color Scanner (CZCS) on board the Nimbus-7 satellite was the first sensor to observe ocean color from space. The CZCS is employed to measure the concentration of phytoplankton pigments in the ocean by measuring the radiance backscattered out of the ocean. In general, the ocean color without pigment will appear blue. This phenomena is due to Rayleigh scattering. On the other hand, the ocean color with pigment will become green. It is due to the absorption of light by pigment. Therefore, the concentration of pigments can be obtained by the change of the ocean color. The understanding of ocean color can be extended to further applications, such as biomass products, mesoscale eddy dynamics, and the variability of ocean current.

ADEOS/OCTS (Advanced Earth Observing Satellite/Ocean Color Temperature Scanner) launched on August 17, 1996 by Japan is another satellite to study ocean color. OCTS has 8 channels in visible and near-infrared and 4 channels in infrared. The principal functions of OCTS are to measure the ocean color and sea surface temperature, to investigate the cyclic circulation of carbon, to exploit the field of fishery, and to monitor the environment. Unfortunately, due to a problem in her solar panels, OCTS is out of commission in June, 1997. SeaWiFS (Sea-viewing Wide Field-of-view) launched on August 1, 1997 by the USA is a new generation operational ocean color satellite. The major functions of SeaWiFS are to estimate the concentration of chlorophyll, and finally to understand the role of ocean in the global climatic changes (Gregg et. al., 1993).

ROCSAT-1 (the first satellite of Republic of China) is scheduled to be launched in 1999 with 35 degrees of orbital inclination, 600-km height and 96.7 minute period. There are three sensors on the platform: Ocean Color Imager (OCI), Ionospheric Plasma and Electrodynamics Instrument (IPEI), and Experimental Communication Payload (ECP). The OCI instrument has seven channels with central wavelengths at 0.443, 0.490, 0.510, 0.555, 0.670, 0.865 and 0.555 μm, labeled Bands 1, 2, 3, 4, 5, 6, and 7, respectively. The Bands 4 and 7 have the same

wavelength. The swath of OCI is about 700 km, with 896 pixels per line. The spatial resolution is fixed at about 800 m. The spectral range and corresponding color of OCI sensors are listed in Table 1. The main functions of OCI are the same as those of SeaWiFS.

Atmospheric correction is described in Section 2. Rayleigh scattering optical depth and radiance are calculated in Section 3. Analyses and discussions of the temporal and spatial variations of Rayleigh scattering optical depth and radiance are then given in Section 4. Section 5 is the conclusions.

2. ATMOSPHERIC CORRECTION

By ignoring direct sun glint and assuming that the sea surface is flat, an algorithm of atmospheric correction for CZCS data has been successfully developed (Gordon, 1976; Gordon, 1978; Gordon and Clark, 1980; Gordon and CastaÒo, 1987; Gordon *et al.*, 1988). The total radiance (I_t) received by CZCS sensors can be expressed as follows

$$I_t = I_r + I_a + t\, I_w \tag{1}$$

where I_r, I_a and I_w represent Rayleigh scattering, aerosol scattering and water-leaving radiances, respectively, and t is diffuse transmittance. In the first stage of development of the algorithm for OCI data, the above algorithm was accepted in this paper. Because OCI sensors have higher radiometric sensitivity than that of CZCS, the variation of optical depth of Rayleigh scattering caused by the deviation of actual sea surface pressure was considered in this paper.

It was found that the amount of pigment is dependent on water-leaving radiance. So, before investigating the amount of pigment, it is necessary to remove the atmospheric effect (including Rayleigh and aersol scattering) from the total radiance. Unfortunately, it is shown that water-leaving radiance is less than 20% of total radiance (Gordon and Wang, 1992). Consequently, if we want to derive accurate water-leaving radiance, we should have accurate Rayleigh radiance and aerosol radiance calculations. In general, Rayleigh radiance can be

Table 1. The characteristics of OCI of ROCSAT-1.

channel	Wavelength (μm)	color	object
1	0.433-0.453	blue	chlorophyll
2	0.480-0.500	blue-greenish	chlorophyll
3	0.500-0.520	green	chlorophyll
4	0.545-0.565	green-yellowish	chlorophyll
5	0.660-0.680	red	aerosol
6	0.845-0.885	red	aerosol
7	0.545-0.565	green-yellowish	chlorophyll

calculated accurately by a theoretical method, but aerosol radiance is determined by experience. According to the magnitude of influence on total radiance, the atmospheric effect was divided into three orders: (1) the zero order, including Rayleigh scattering, Mie scattering of heavy concentration of aerosol, (2) the first order, including Mie scattering; water-leaving radiance has the same magnitude as the first order of atmospheric effect, but the actural magnitude is dependent on the wavelength of incident light. (3) the second order, including the effects of multiple scattering, polarization, roughness of sea surface and view angle and the spatial and temporal variation of pressure and total amount of ozone.

It is evident that the primary influence on ocean color remote sensing is Rayleigh scattering and the secondary influence is Mie scattering. In this study, the calculation of Rayleigh scattering was focused on.

3. RAYLEIGH SCATTERING OPTICAL DEPTH AND RADIANCE

For single scattering approximation Rayleigh radiance, $I_r(\lambda)$, can be expressed as follows

$$I_r(\lambda) = \frac{\tau_r(\lambda) F_0(\lambda) P_a}{4\pi \cos\theta} \tag{2}$$

where $\tau_r(\lambda)$ is the Rayleigh scattering optical depth under different pressure, P ; $F_0(\lambda)$ is solar flux with atmospheric attenuation; P_a is the probability of light scattered to sensor; θ is the zenith angle of satellite.

In (2) the parameters of $F_0(\lambda)$, P_a, $\cos\theta$ are known for a given geometry, and the only variable is $\tau_r(\lambda)$. Hansen and Travis (1974) showed that under standard sea surface pressure, P_o, Rayleigh scattering optical depth, τ_{or}, can be expressed as follows

$$\tau_{or}(\lambda) = 0.008569\,\lambda^{-4}(1+0.0113\,\lambda^{-2}+0.00013\,\lambda^{-4}) \tag{3}$$

where λ is wavelength in μm unit . Table 1 is the listing of the Rayleigh scattering optical depth for OCI 6 channels under standard sea surface pressure. It was found that the shorter wavelength and the less small optical depth, and the magnitude of optical depth is approximately inversely proportional to the fourth power of wavelength.

Considering the effect of the deviation of sea surface pressure on Rayleigh scattering optical depth, the responsible Rayleigh scattering optical depth should be adjusted as follows

$$\tau_r(\lambda) = \tau_{or}(\lambda) P/P_o \tag{4}$$

where P is the actual sea surface pressure, which can be obtained by ground station observations and the following hydrostatic equation

$$P = P_{sta}\left(1+\gamma\, Z/T_{sta}\right)^{g/R\gamma} \tag{5}$$

where R (287 J/mole.K) is gas constant , γ (0.0065 K/m) is the actual temperature lapse rate , P_{sta} ,T_{sta} , and Z are the observed pressure, temperature and level height of ground station.

4. RESULT ANALYSIS

4.1 Temporal and Spatial Variations of Rayleigh Scattering Optical Depth

The purpose of the OCI science team is to establish an operational model for real time data processing. Therefore, it is very important to establish a fast and effective atmospheric model to perform the atmospheric correction. For operational purposes, the oceans around Taiwan are divided into 5 regions as shown in Figure 1. For each region the Rayleigh scattering optical depth variations with time were analyzed. Region 1 ranges from 24.83°N to 26.35°N

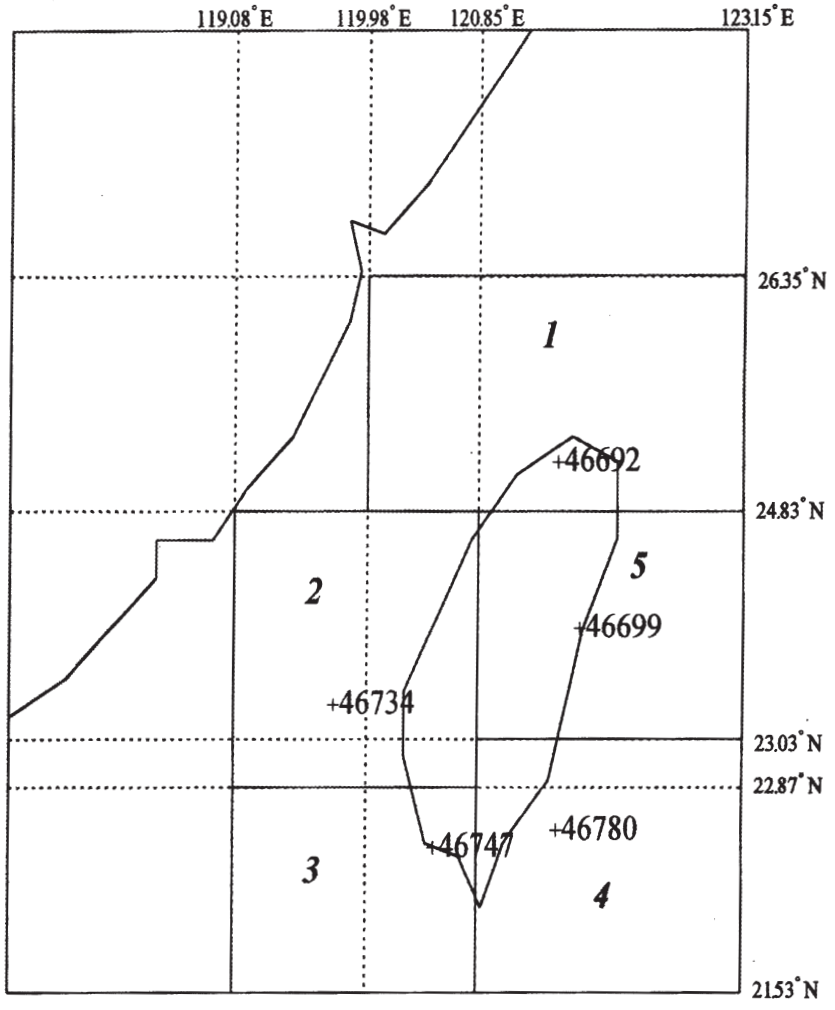

Fig. 1. The distribution of the five ground stations near the coast in the Taiwan area. They are Pan-Chiao station, coded number (46692), Tung-Kang (46747), Ma-Kung (46734), Green Island (46780) and Hua-Lien (46699).

in latitude and from 119.98°E to 123.15°E in longitude. Pan-Chiao ground station, coded number 46692, was selected as the representative of region 1. The sea level pressure was calculated by (5) using ground pressure measurements and then Rayleigh scattering optical depth was obtained from (4). Figure 2 is the three-year (from 1993 through 1995) series of the Rayleigh scattering optical depth for OCI channel 1 at region 1. It is found that the Rayleigh scattering optical depth has a significant temporal variation during a one year period. The maximum value is in the winter and the minimum is in the summer. Actually, the situation is the same as in pressure variation by seasons. The heavy curve in Figure 2 is the curve fitting for Rayleigh scattering optical depth. It looks like a parabolic curve. Figure 3 is the same as Figure 2, but for OCI channel 6. Comparing with Figure 2, it was found that both have the same pattern, but the magnitude of Rayleigh scattering optical depth of OCI channel 1 is larger than that of channel 6. Figure 4 is the Rayleigh scattering optical depth fitting curves for OCI channel 1 at six different regions. It is shown that, except in region 4, the tendency of the Rayleigh scattering changing by season is quite significant. Generally the magnitude in order are region 1, region 5, region 3, region 2 and region 4; but, region 1, region 5 and region 3 have little difference in the summer.

4.2 Rayleigh Scattering Optical Depth Model

For the purpose of real time operation, it is necessary to establish a fast and effective model to provide Rayleigh scattering optical depth. Table 2 lists the regression coefficients of Rayleigh scattering optical depth for OCI six channels at region 1. If there is a ground observation of region 1, its Rayleigh scattering optical depth can be obtained by equations (4) and (5). If there is no ground observation, its Rayleigh scattering optical depth can be derived by the Rayleigh scattering model. The model inputs are the wavelength and day of year.

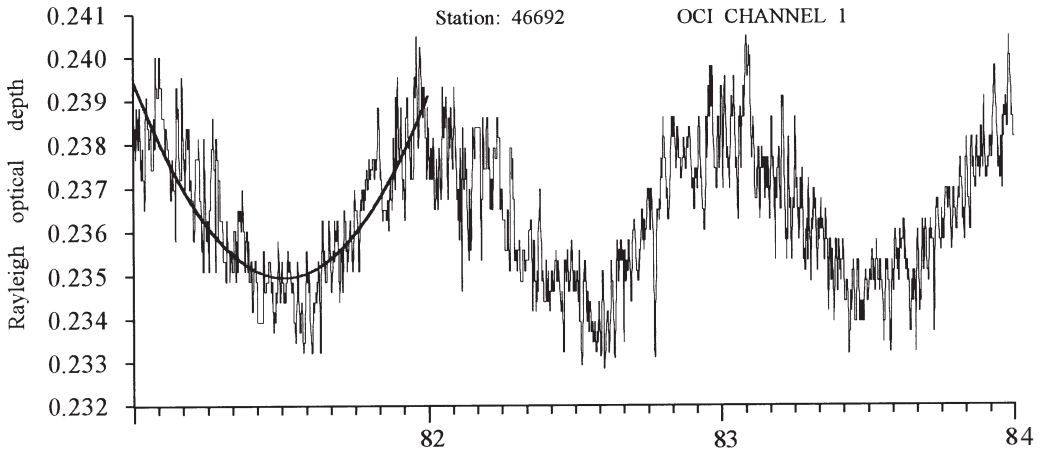

Fig. 2. The variation of Rayleigh scattering optical depth channel 1 for the OCI channel 1 from 1993(82) though 1995(84) using the Pan-Chiao ground station data.

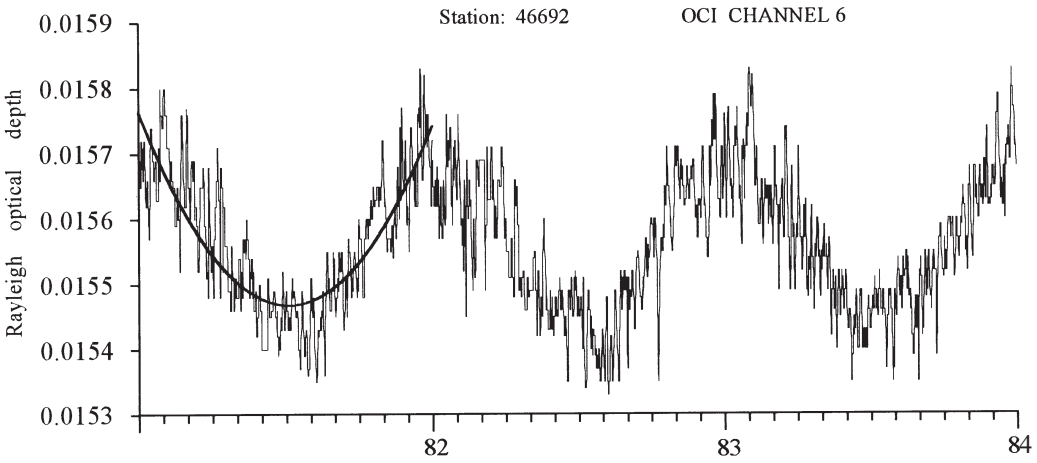

Fig. 3. Same as Figure 2, but for the OCI channel 6.

Table 3 is the error analysis of Rayleigh scattering radiance for OCI 6 channels using the dependent data (1993) and independent data (1994 and 1995) as checking points. It is shown that in the Pan-Chiao, area the root mean square errors between the regression estimated values and actual values are quite small for each channel. Thus, the estimated values are reasonable and usable when measured data are absent.

4.3 Seasonal Variation of Rayleigh Scattering Radiance

Figure 5 shows the simulated image of Rayleigh scattering radiance from 0809:48 LST, January 1, 1997 to 0811:31.8 LST for OCI channel 1. The range of the image is 114.63~117.92° E and 17.24~22.73° N. It shows that the distribution of Rayleigh scattering radiance is symmetric about the satellite track, that the range of radiance is from 3.524 to 4.766 mW/cm^2 -μm-sr, and that the smaller region is near the satellite track and increases with zenith angle. To investigate the Rayleigh scattering pattern with time, five images are simulated every two hours from 0810LST to 1610LST. It was found that before noon, the minimum regions are moving from the nadir to edge and after noon, the situation is the reverse. This change of pattern is caused by the relative position between satellite and the sun and solar zenith angle. The smaller the solar zenith angle is, the stronger the backscattering radiance is.

In addition, the seasonal variation of Rayleigh scattering radiance was investigated by twelve simulated images. The date and the time of first image are at 0810 LST of January 1 1997, and the date and time of the others are same as first image but in different months, from February to December. Comparing the twelve images, it was found that the Rayleigh scattering radiance is mainly changed with solar declination, that is, the Rayleigh scattering radiance is smaller in the winter and larger in the summer. Table 4 is the daily and seasonal variations of Rayleigh scattering radiance. It was shown that in daily variation the maximum is at 0810LST, and the minimum at 1010 LST and both the minimum and the maximum are decreasing with

time after noon. It is also noted that the difference between minimum and maximum is at 0810 LST.

5. CONCLUSIONS

The key problem for ocean color investigation using Ocean Color Imager radiance is the correction of atmospheric effects. In particular, the water-leaving radiance is an order of magnitude less than that of observed radiance, so the accuracy of the concentration of phytoplank-

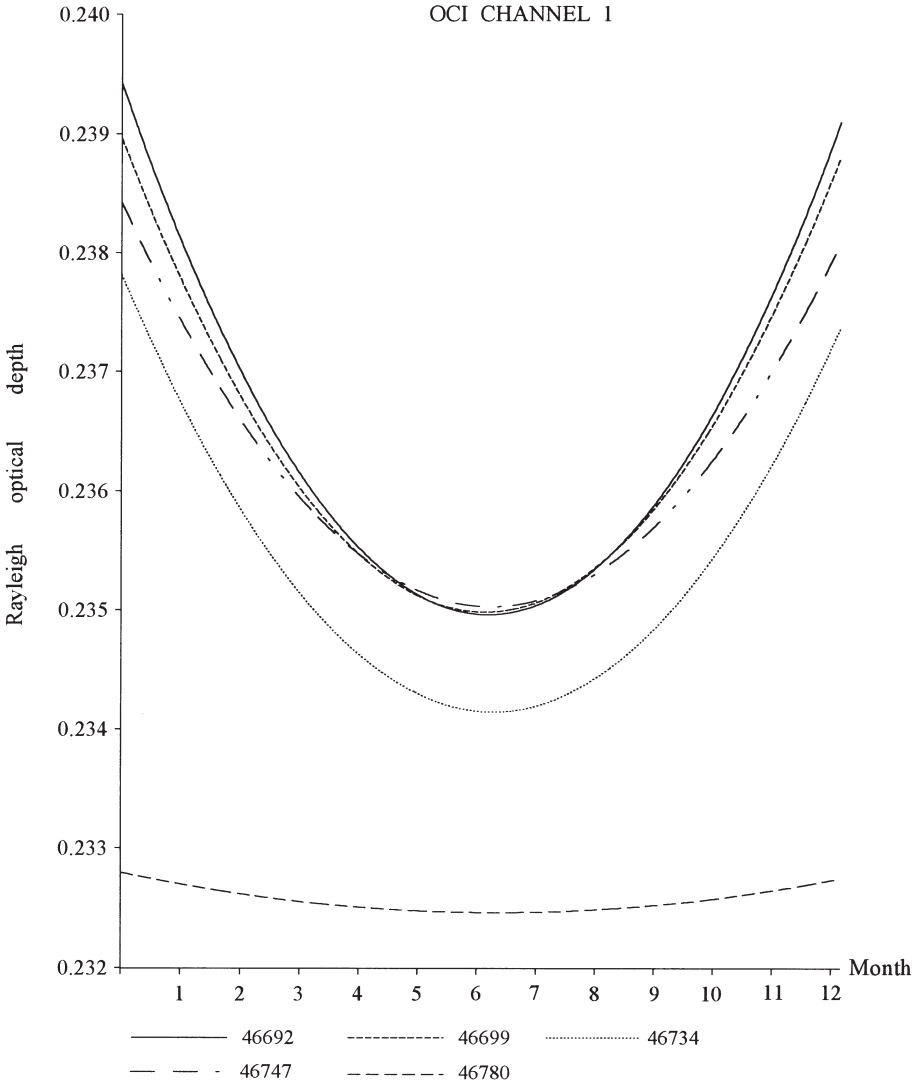

Fig. 4. The Rayleigh scattering optical depth fitting curves for OCI Channel 1 at six different regions.

Table 2. At Pan-Chiao area for OCI 6 channels, the coefficients of 2 order polynomial fitting curve, τ (D)= $a_0 + a_1 D + a_2 D^2$, where D is the day of year.

CHANNEL	a_0	a_1	a_2
1	0.2394437	-2.4071798E-05	3.2317296E-08
2	0.1582137	-1.5904736E-05	2.1352843E-08
3	0.1343105	-1.3505147E-05	1.8130939E-08
4	9.50979E-02	-9.5621299E-06	1.2837059E-08
5	4.42469E-02	-4.4444873E-06	5.9675456E-09
6	1.57642E-02	-1.5884950E-06	2.1331432E-09

Table 3. At Pan-Chiao area for OCI 6 chammels, the root mean square error between regression estimated Rayleigh scattering radiance and actual Rayleigh scattering radiance.

		Station				
Year	CHANNEL	46692	46699	46734	46747	46780
1993	CH 1	.0043352552	.0043244214	.0043582298	.0044889153	.0017749284
	CH 2	.0012836211	.0012009455	.0009896762	.0008882014	.0026311613
	CH 3	.0013330192	.0012968325	.0012435140	.0012720686	.0013543617
	CH 4	.0014063672	.0013966322	.0013995819	.0067865805	.0006741824
	CH 5	.0004931478	.0004716524	.0004100706	.0003704254	.0009780343
	CH 6	.0001316327	.0001252759	.0001126313	.0001117941	.0001978786
1994	CH 1	.0048924936	.0048684219	.0047743559	.0047512310	.0021515880
	CH 2	.0012458681	.0011767420	.0010590304	.0010524947	.0024049694
	CH 3	.0015630690	.0015311072	.0014575207	.0014420306	.0012539715
	CH 4	.0016166876	.0016035237	.0015632832	.0064955652	.0007409450
	CH 5	.0004178815	.0003993385	.0003742365	.0003781294	.0009063966
	CH 6	.0001492434	.0001440610	.0001337476	.0001322924	.0001800870
1995	CH 1	.0046662164	.0045594587	.0045401570	.0044154807	.0022597634
	CH 2	.0011400785	.0010701461	.0009305644	.0008500601	.0022434330
	CH 3	.0014286743	.0013580607	.0013110107	.0012234678	.0011535158
	CH 4	.0015242669	.0014792264	.0014666217	.0060467335	.0007395576
	CH 5	.0004165854	.0004102371	.0003724815	.0003723244	.0008593269
	CH 6	.0001341487	.0001255090	.0001165322	.0001059202	.0001657099

ton pigments retrieval depends on the accuracy of the correction of atmospheric effect. Rayleigh scattering— the zeroth order atmospheric correction is the focus of this paper. The results show that the Rayleigh scattering and transmittance change significantly for various locations and seasons. To make sure that the atmospheric model can be used in operation, a model for providing Rayleigh scattering optical thickness and transmittance has been established, using three-year ground weather surface data.

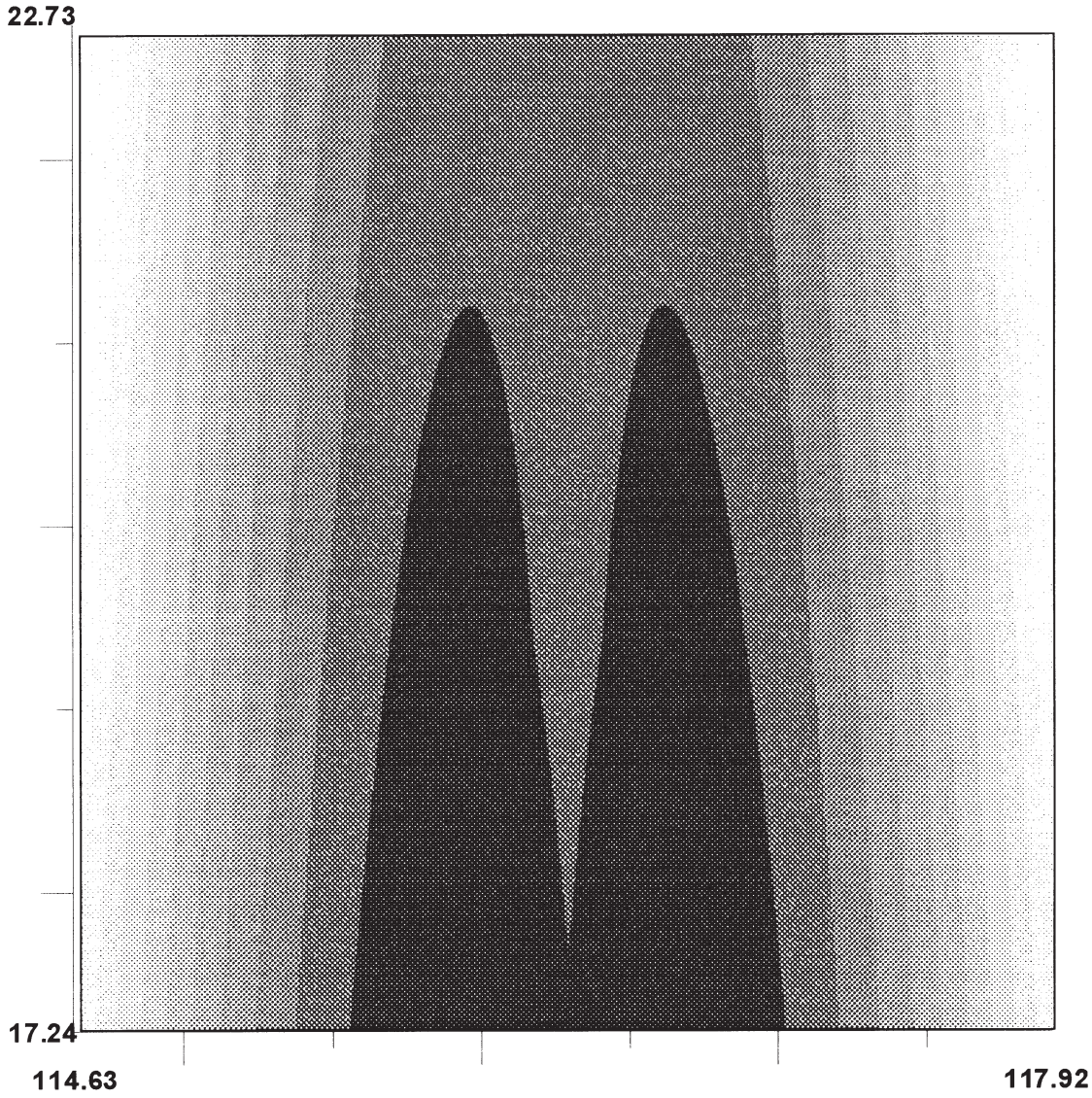

Fig. 5. The simulated image of Rayleigh scattering radiance. The scan time of simulated image is from 0809:48 LST, January 1 1997 to 0811:31.8 LST. The scan range is 114.63 ~ 117.92°E and 17.24 ~ 22.73°N. The dark color represents low radiance and the light color represents high radiance.

In daily variation, the results show that before noon the minimum regions of Rayleigh scattering radiance spread from the center to the edge in the Rayleigh radiance image and after noon the minimum regions of Rayleigh scattering radiance come together from the edge to the

Table 4. At Pan-Chiao area for OCI channel 1, the daily and seasonal variation of Rayleigh scattering in mW/cm^2 - μm-sr unit.

year	month	day	hour	minimum	maximum	difference
1997	1	1	8	3.52480	4.76619	1.24139
	1	1	10	3.46594	3.94706	0.48112
	1	1	12	3.71906	4.42309	0.70403
	1	1	14	3.69795	4.12413	0.42618
	1	1	16	3.55695	4.23283	0.67588
	2	1	12	3.87896	4.65559	0.77643
	3	1	12	4.21945	5.01479	0.79534
	4	1	12	4.76054	5.34789	0.58735
	5	1	12	5.22931	5.44920	0.21989
	6	1	12	5.39591	5.51179	0.11588
	7	1	12	5.35354	5.49953	0.14599
	8	1	12	5.25883	5.38259	0.12376
	9	1	12	4.89974	5.34332	0.44358
	10	1	12	4.43506	5.13287	0.69781
	11	1	12	4.00141	4.76436	0.76295
	12	1	12	3.76055	4.47438	0.71383

center. The reason for these phenomena may be caused by different solar zenith angles. As to seasonal variation, when the variations of 12 images of Rayleigh scattering radiance are compared with one another, it is found that the Rayleigh scattering radiance was significantly changed following the movement of declination of sun. Generally, the Raleigh scattering radiance in winter is less than that in summer. In addition, the minimum value, the maximum value and the range of Rayleigh scattering radiance were discussed. In daily variation, the results show that among the maxima, the radiance at 8 A.M. is the largest, and among the minima, the radiance at 10 A.M. is the smallest, and that within the range the difference at 8 A.M. is the largest, and at 10 A.M. is the smallest. In seasonal variation, the results show that among the minima, January is largest and among the maxima, June is the smallest. The Rayleigh scattering radiance regularly increases from January to June and regularly decreases from June to December and the minimum range occurs in March and maximum range in June.

Acknowledgements The authors are grateful to three anonymous reviewers for their helpful comments on the manuscript. This work was supported by the National Science Council, National Space Program Office, Republic of China, under the contract NSC 86-NSPO-A-OCI-019-01-02.

REFERENCES

Gordon, H. R., 1976: Radiative transfer: A technique for simulating the ocean in satellite remote sensing calculations. *Appl. Opt.*, **15**, 1974-1979.

Gordon, H. R., 1978: Removal of atmospheric effects from satellite imagery of the oceans. *Appl. Opt.*, **17**, 1631-1636.

Gordon, H. R. and D. K. Clark, 1980: Atmospheric effects in the remote sensing of phytoplankton pigments. Bound. *Layer Meteor.*, **18**, 299-313.

Gordon, H. R. and D. J. CastaÒo, 1987: The coastal zone color scanner atmospheric correction algorithm: multiple scattering effects. *Appl. Opt.*, **26**, 2111-2122.

Gordon, H. R. and D. J. CastaÒo, 1988: The coastal zone color scanner atmospheric correction algorithm: influence of El ChichÛn. *Appl. Opt.*, **27**, 3319-3321.

Gordon, H. R., J. W. Brown and R. H. Evans, 1988: Exact Rayleigh scattering calculations for use with the Nimbus-7 Coastal Zone Color Scanner. *Appl. Opt.*, **27**, 862-871.

Gordon, H. R. and M. Wang, 1992: Surface-roughness considerations for atmospheric correction of ocean color sensors. II. Error in the retrieved water-leaving radiance. *Appl. Opt.*, **31**, 4261-4267.

Gregg, W. W., F. C. Chen, A. L. Mezaache, J. D. Chen and J. A.Whiting, 1993: The simulated SeaWiFS data set version 1. *NASA Technical Memorandum* 104566, **9**, pp19.

Hansen, J. E. and L. D. Travis,1974: Light scattering in planetary atmosphere. *Space Sci. Rev.*, **16**, 527.